Deficiency of the *ywhaz* gene, involved in neurodevelopmental disorders, alters brain activity and behaviour in zebrafish

Antón-Galindo E[1,2,3,4]*, Dalla Vecchia E[5]*, Orlandi JG[6], Castro G[7], Gualda E[7], Loza-Alvarez P[7], Aguado F[8], Norton WHJ[5#], Cormand B[1,2,3,4#], Fernàndez-Castillo N[1,2,3,4#]

[1]Departament de Genètica, Microbiologia i Estadística, Facultat de Biologia, Universitat de Barcelona, Barcelona, Spain

[2]Centro de Investigación Biomédica en Red de Enfermedades raras (CIBERER), Spain

[3]Institut de Biomedicina de la Universitat de Barcelona (IBUB), Barcelona, Spain

[4]Institut de recerca Sant Joan de Déu (IRSJD), Espluges de Llobregat, Spain

[5]Department of Neuroscience, Psychology and Behaviour, College of Life Sciences, University of Leicester, Leicester, UK

[6]RIKEN Center for Brain Science, Wako-shi, Saitama 351-0198, Japan

[7]The Institute of Photonic Sciences, (ICFO) Castelldefels (Barcelona), Spain

[8]Department of Cell Biology, Physiology and Immunology, University of Barcelona; Institute of Neurosciences, UB; Barcelona, Spain.

* equally contributed to this work; # equally supervised this work

ABSTRACT

Genetic risk variants in *YWHAZ*, encoding 14-3-3ζ, have been found to contribute to psychiatric disorders such as autism spectrum disorder and schizophrenia, and have been related to an impaired neurodevelopment in humans and mice. Here, we have used a zebrafish model to further understand the mechanisms by which *YWHAZ* contribute to neurodevelopmental disorders. We first observed pan-neuronal expression of *ywhaz* during developmental stages, suggesting an important role of this gene in neural development. During adulthood *ywhaz* expression was restricted to Purkinje cells in the cerebellum, a region that shows alterations in autistic patients. We then established a novel stable *ywhaz* knockout (KO) zebrafish line using CRISPR/Cas9 genome engineering. We performed whole-brain calcium imaging in wild-type (WT) and *ywhaz* KO larvae and found altered neural activity and functional connectivity in the hindbrain. Interestingly, adult *ywhaz* KO fish also display decreased levels of dopamine and serotonin in the hindbrain and freeze when exposed to novel stimuli, a phenotype that can be reversed with fluoxetine and quinpirole, drugs that target serotonin and dopamine neurotransmission. Together, these findings suggest an important role for *ywhaz* in establishing neuronal connectivity during developmental stages. *ywhaz* deficiency leads to impaired dopamine and serotonin neurotransmission that may underlie the altered behaviour observed during adulthood.

INTRODUCTION

The 14-3-3 gene family codes for a highly conserved group of molecular chaperones that play important roles in biological processes and neuronal development [1]. *YWHAZ*, encoding 14-3-3ζ, is involved in neurogenesis and neuronal migration, as shown by morphological changes in the brain of 14-3-3ζ knockout mice [2–5]. These animals present behavioural alterations, that have been related to psychiatric disorders, such as schizophrenia [2, 5], including hyperactivity, impaired memory, lower anxiety and impaired sensorimotor gating.

Several studies have pointed to an association between Y*WHAZ* and psychiatric disorders. In a previous study, we found that a frameshift mutation in the *YWHAZ* gene, inherited from a mother with depression, had functional implications in two siblings diagnosed with autism spectrum disorder (ASD) and attention deficit/hyperactivity disorder (ADHD) [6]. In addition, genetic studies have associated *YWHAZ* polymorphisms to major depression and schizophrenia [6, 7]. Finally, decreased expression of the *YWHAZ* gene and 14-3-3ζ protein was reported in post-mortem brains of ASD and schizophrenia patients [6, 8, 9], and 14-3-3 protein levels are reduced in platelets and pineal glands of ASD patients [10, 11]. However, the mechanisms by which *YWHAZ* contributes to neurodevelopmental disorders remain unclear.

The zebrafish is a powerful model to study neurodevelopmental and psychiatric disorders due to several advantages. Firstly, zebrafish present a high genetic similarity to humans and are easy to manipulate genetically. Secondly, they display well-defined behaviours that can be translated to humans in some cases. Lastly, their small size and transparency during larval stages make zebrafish ideal for *in vivo* imaging studies [12, 13]. Indeed, whole-brain imaging is a recently developed technique that allows *in vivo* neuronal activity and connectivity to be investigated [14, 15]. This novel approach combined with genetic engineering stands as an excellent tool to use in specific zebrafish models to study the neural basis of human brain disorders.

In this study, we aim to investigate the role of *YWHAZ* in brain development and function using a novel mutant line. We explore the effect of loss of *ywhaz* function on neural activity and connectivity during development, and in neurotransmission and behaviour during adulthood.

MATERIAL AND METHODS

Zebrafish strains, care and maintenance

Adult zebrafish and larvae (*Danio rerio*) were maintained at 28.5°C on a 14:10 light-dark cycle following standard protocols. All experimental procedures were approved by a local Animal

Welfare and Ethical Review board (University of Leicester and Generalitat de Catalunya). AB wild-type (WT), *Tg*(*aldoca:gap43-Venus*), *Tg*(*olig2*:*egfp*)^{vu12}, *ywhaz*$^{-/-}$, albino *Tg(elavl3:GCaMP6s)* and albino *Tg(elavl3:GCaMP6s)ywhaz*$^{-/-}$ zebrafish lines were used for the experiments.

In situ hybridization (ISH) and immunohistochemistry (IHC)

A specific mRNA probe targeting *ywhaz* (NCBI Reference Sequence: NM_212757.2) was prepared and ISH experiments were performed in larvae and dissected adult brains of AB wild-type (WT), *Tg*(*aldoca:gap43-Venus*), *Tg*(*olig2*:*egfp*)^{vu12} and *ywhaz*$^{-/-}$ zebrafish strains. IHC was performed in adult *Tg*(*olig2*:*egfp*)^{vu12}, *ywhaz*$^{-/-}$ and *Tg*(*aldoca*:*gap43-Venus*)^{rk22} brains. Details of the procedures are described in the Supplementary methods.

Generation *ywhaz* zebrafish knock out using CRISPR/Cas9

The detailed CRISPR/Cas9 targeted mutagenesis protocol is described in the Supplementary methods. A synthetic guide RNA (sgRNA) targeting exon 3 of *ywhaz* was designed and cloned into the pDR274 vector (Addgene plasmid #42250) [16]. The sgRNA was transcribed using the mMESSAGE mMACHINE Kit (Life Technologies). Cas9 mRNA was transcribed *in vitro* from the pMLM3613 vector (Addgene plasmid #42251, Keith Joung) [16] using the mMESSAGE mMACHINE T7 Ultra Kit (Life Technologies). To generate the mutants, 1 nl total volume of a mixture of 25 ng/µl sgRNA and 250 ng/µl Cas9 mRNA was injected to one-cell stage embryos to form the F0 generation. Once a F0 fish carrying an interesting indel transmitted to the germline was identified, the F1 embryos born from a cross between the selected F0 founder and AB WT were raised to adulthood, screened for the mutation of interest, and subsequently in-crossed to obtain a final stable F2 homozygous mutant line.

Gene expression analysis using Real-Time quantitative PCR (RT-qPCR)

Total RNA was extracted from the whole brains of WT and *ywhaz*$^{-/-}$ adult zebrafish and RT-qPCR was performed on 10 brains per genotype with three replicates as described in the Supplementary methods.

Whole-brain imaging

Light sheet microscopy

Whole-brain imaging experiments were performed on 6 days-post-fertilization (dpf) albino *Tg(elavl3:GCaMP6s)* and *Tg(elavl3:GCaMP6s)ywhaz*$^{-/-}$ zebrafish larvae. Larvae were first paralyzed for 10 minutes in a 1 mg/ml α-bungarotoxin solution (Thermofisher). They were subsequently placed inside a fluorinated ethylene-propylene (FEP) tube (0.7 mm inner diameter), with water and E3 medium, and then into a custom-made chamber to orientate the

larvae appropriately towards the objective of the light-sheet microscope (see Supplementary methods and Figure 1).

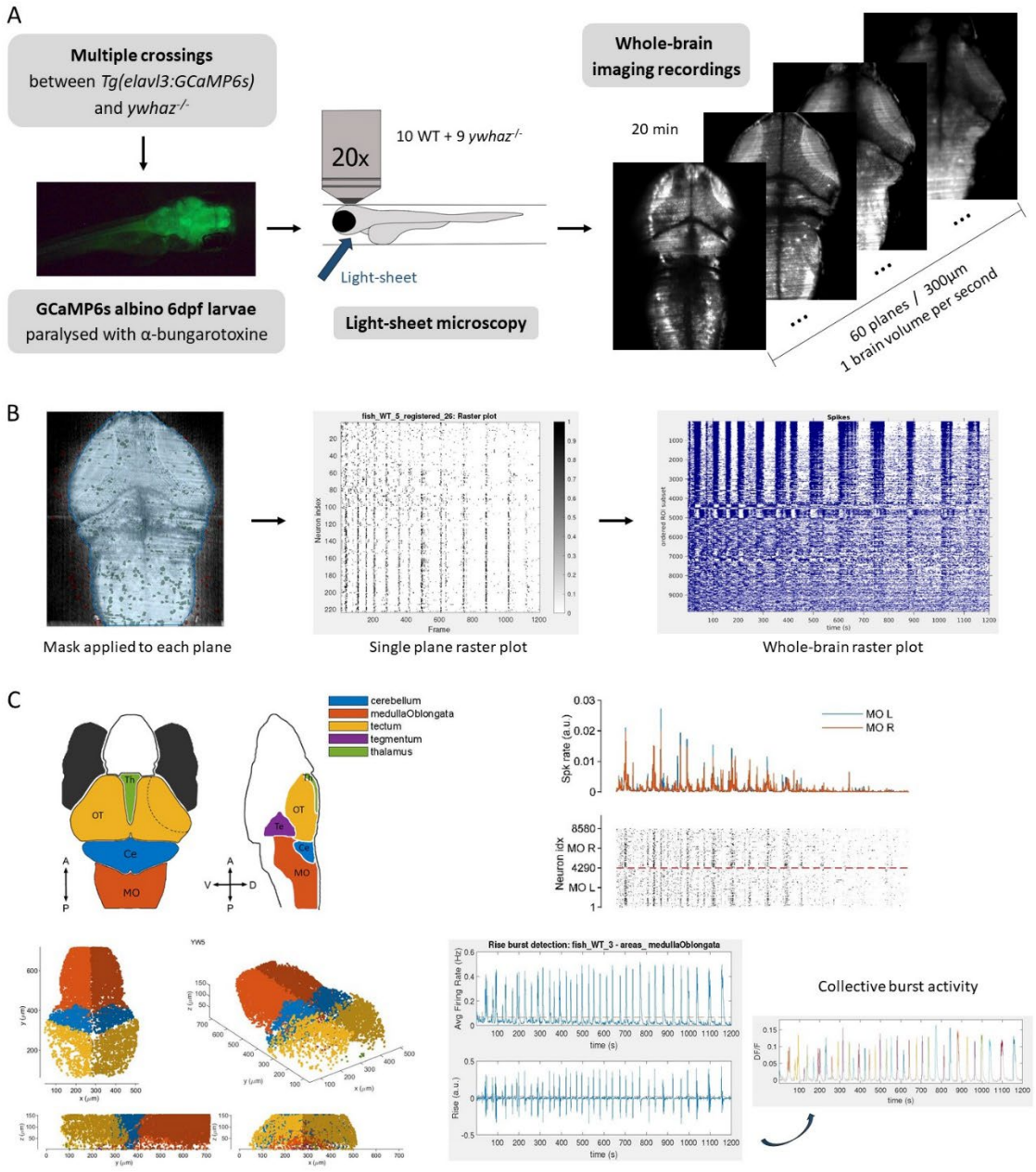

Figure 1. Whole-brain imaging methods. (A) Steps followed to perform the whole-brain imaging recordings in 6 days post-fertilization (dpf) larvae expressing GCaMP6s pan-neuronally. **(B)** Steps followed in the single-cell fluorescence traces extraction. First, a mask was applied to each single plane to avoid detection of fluorescence outside of the brain. Then, single cell fluorescence traces were extracted for all the neurons detected in each single plane. Finally, results from single planes were combined to obtain neuronal activity from the whole-brain of each individual during the 20min recording. ROI, region of interest. **(C)** On the left, brain regions explored in the analysis and plot of all the neurons detected in each brain area of one individual. In a first approach, we divided the three biggest regions (Ce, OT, and MO) by hemispheres and obtain no differences in the number of neurons or activity between hemispheres (top right). After analysing single-cell activity, we inspected collective burst activity in each of the five defined brain areas (bottom right). Ce, cerebellum; MO, medulla oblongata; OT, optic tectum; Te, tegmentum; Th, thalamus.

Image segmentation and extraction of calcium signals

To extract ΔF/F traces from our calcium imaging recordings, we followed the CaIman MATLAB pipeline [17]. First, volumetric data were motion corrected and separated into time series for each imaged plane. Then, individual planes were processed using constrained non-negative matrix factorization method (CNMF) [18]. We overestimated the number of ROIs, as the program discards ROIs during the refinement process, and applied a mask to avoid signal detection outside the brain. The data from each plane were then combined to produce a single dataset for an imaged larva (Figure 1).

Activity and functional connectivity analysis

We used Netcal (www.itsnetcal.com) to analyse fluorescence data and obtain single-cell and collective level statistics. To perform the analysis in different areas of the brain, we used MATLAB Volume Segmenter and the Z-brain atlas as a reference (http://engertlab.fas.harvard.edu/Z-Brain/) to delimitate five brain regions: thalamus, tegmentum, optic tectum, cerebellum and medulla oblongata (MO). We also performed analysis of network connectivity inside each of the delimited areas (Figure 1).

High precision liquid chromatography (HPLC) analysis of monoamines and metabolites

Fish were decapitated and their brains were dissected and divided into four areas: telencephalon (Tel), diencephalon (DI), optic tectum (TeO) and hindbrain (Hb). HPLC analysis for dopamine (DA), serotonin (5-HT), 3,4-dihydroxyphenylacetic acid (DOPAC), and 5-hydroxyindoleacetic acid (5-HIAA) was carried out using electrochemical detection [19] as described in the supplementary methods.

Behavioural tests

A battery of behavioural tests was performed in adult zebrafish (3-5 months-old) mixed groups of both sexes. Two tests to assess social behaviour were also performed on juvenile (one month-old) zebrafish. All fish were genotyped, sized-matched and maintained in groups of 15 by genotype until the day of testing. Methodological details of the tests performed are described in the Supplementary Methods.

Drug treatments

Fluoxetine 5 mg/L diluted in DMSO (Tocris #0927) was administered by immersion for 2 hours. Quinpirole 0.25-4 mg/L diluted in H_2O (Tocris #1061) was administered by immersion for 1 hour.

Statistical methods

Statistical analysis of RT-qPCR, HPLC and behavioural data were performed in GraphPad Prism 6. The data sets were assessed for normality using D'Agostino-Pearson and Shaphiro-Wilk normality test. Either a Mann-Whitney or an unpaired t-test whit Welch's correction was performed to compare two groups, with corrections for multiple comparisons when needed. Statistical methods used for the brain imaging analysis are detailed in the Supplementary Methods.

RESULTS

Expression of *ywhaz* during development and adulthood in WT zebrafish

We first investigated *ywhaz* expression in the developing brain. In two to nine dpf WT larvae, *ywhaz* expression is widespread covering almost all brain areas, with a particularly strong signal in the cerebellum of whole mount embryos (Figure 2A). In contrast, in adult zebrafish, *ywhaz* expression is restricted to the cerebellum. *ywhaz* was present in the granule cell layer (GCL) of the valvula cerebelli (Va) and crista cerebellaris (CCe), most likely within the Purkinje cell layer (PCL) (Figure 2B).

We next combined *ywhaz* ISH with an anti-GFP antibody stain on adult brain sections of *Tg*(*aldoca:gap43-Venus*) [20] and *Tg*(*olig2*:*egfp*)^{vu12} [21] transgenic lines, to confirm that *ywhaz* is expressed only within Purkinje cells and not in Eurydendroid cells, the zebrafish equivalent of the deep cerebellar nuclei in humans [22]. In the *Tg*(*aldoca:gap43-Venus*) line, the promoter of the *aldolase Ca* (*aldoca*) gene [20] is used as a driver and EGFP labels Purkinje cells, inhibitory neurons in the PCL. In the *Tg*(*olig2*:*egfp*)^{vu12} fish cerebellum, EGFP labels Eurydendroid cells [21], excitatory neurons that are situated ventrally to Purkinje cells [23]. We found that *ywhaz* ISH staining overlaps GFP in the *Tg*(*aldoca:gap43-Venus* line), meaning that *ywhaz* is expressed within Purkinje cells and not within Eurydendroid cells at adult stages (Supplementary Figures 1 and 2).

Generation of a *ywhaz*$^{-/-}$ zebrafish mutant line by CRISPR-Cas9 mutagenesis

We next generated a novel *ywhaz* mutant line, as a first step towards understanding the function of this gene in neural development. We used CRISPR/Cas9 to engineer a mutation within the third exon of *ywhaz*. We selected a F0 fish carrying a 7 bp deletion (380_387delCCTGGCA) as a founder to generate a stable *ywhaz* mutant line (Supplementary Figures 3 and 4). This deletion

causes a frameshift that leads to a premature stop codon in the third exon of the unique *ywhaz* isoform. The F1 embryos born from the cross between the F0 founder and WT were raised to adulthood, genotyped, and only the F1 fish carrying the 7 bp deletion were kept (Supplementary Figure 4B).

To check whether the 7 bp deletion triggers mRNA degradation by nonsense-mediated mRNA decay (NMD) [24] we analysed *ywhaz* mRNA levels by RT-qPCR. We observed a significantly decreased level of *ywhaz* expression in *ywhaz*$^{-/-}$ compared to WT ($p < 0.0001$, Mann-Whitney U test, Supplementary Figure 5), which suggests that NMD degradation of the truncated *ywhaz* transcript has occurred in mutants. In addition, ISH performed in larvae and adult brains confirmed loss of *ywhaz* expression in the brain of *ywhaz*$^{-/-}$ fish, at both developmental and adult stages (Figure 2C and D).

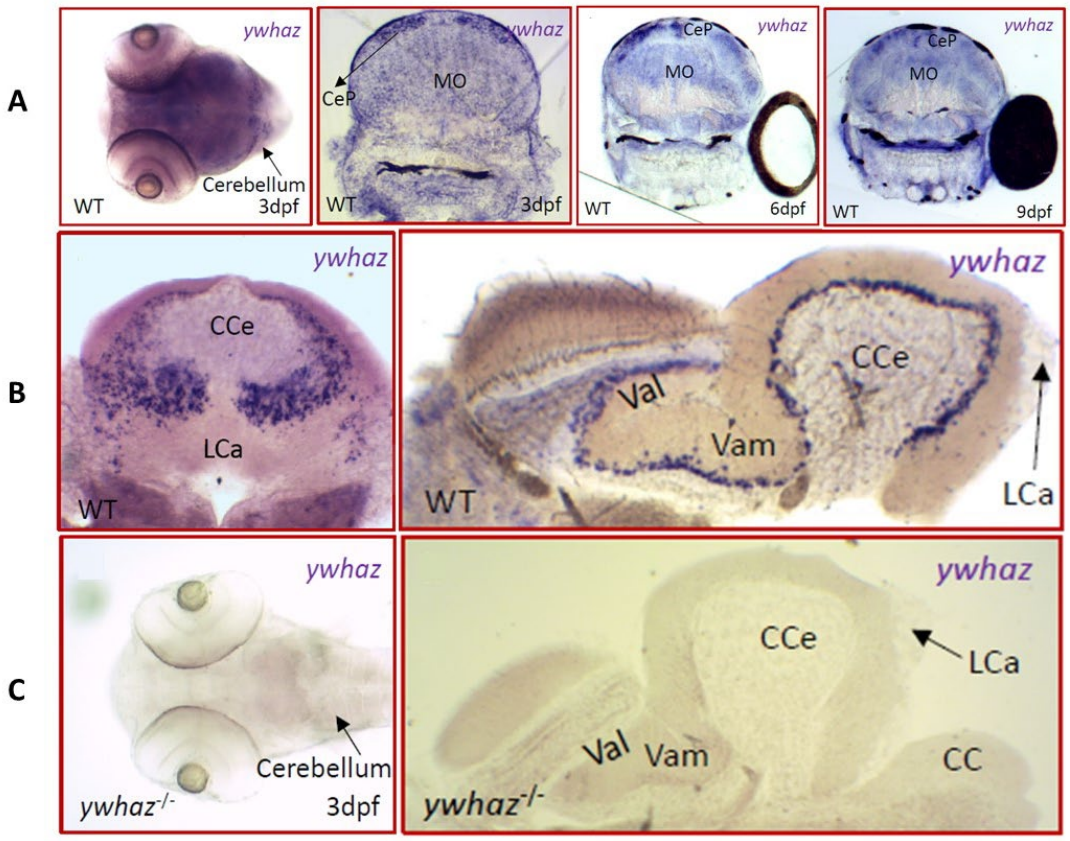

Figure 2. Expression of *ywhaz* in zebrafish during development and adulthood in WT and KO. (A) In WT larvae, *ywhaz* expression is widespread covering almost all brain areas, with a strongest signal in cerebellum. (B) In WT adult brains, *ywhaz* expression is restricted to the granule cell layer in the cerebellum. (C) *ywhaz* is not expressed in *ywhaz*$^{-/-}$ embryos and *ywhaz*$^{-/-}$ adult brains. CC, crista cerebellaris; CCe, corpus cerebelli; CeP, cerebellar plate; LCa, lobus caudalis cerebelli; MO, medulla oblongata; Val, lateral valvula cerebelli; Vam, medial valvula cerebelli.

Altered spontaneous neuronal activity and functional connectivity in the hindbrain of *ywhaz*$^{-/-}$ larvae

The expression pattern of *ywhaz* suggests that it may play an important role during neural development. We performed whole-brain imaging at 6 dpf to investigate changes in neural circuit function and connectivity.

When we compared WT and *ywhaz*$^{-/-}$ larvae we identified differences in hindbrain spontaneous activity and functional connectivity between genotypes. We found an increased number of active neurons in medulla oblongata (MO) of *ywhaz*$^{-/-}$ fish (p = 0.046, Figure 3A), which represent a higher fraction of total active neurons (p = 0.005, Figure 3C). Also, *ywhaz*$^{-/-}$ fish cerebellar neurons represented a lower fraction of total neurons (p = 0.018, Figure 3C). In thalamus and tegmentum, the low number of active neurons that we could detect prevented us from properly assessing activity and connectivity in these areas (Figure 3B and D).

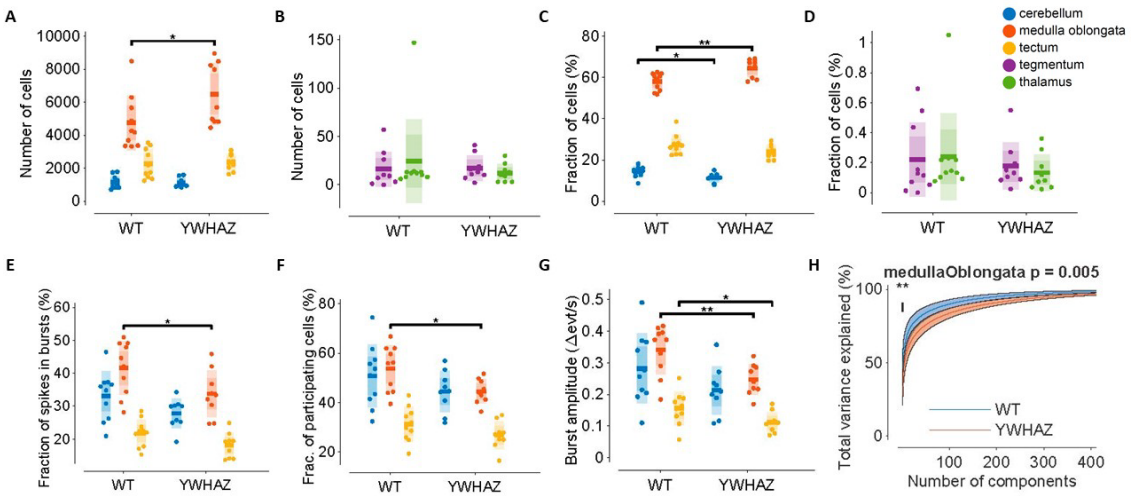

Figure 3. Alterations in neuronal activity in zebrafish *ywhaz*$^{-/-}$ larvae. (A and B) Number of active neurons detected in each brain area. (C and D) Fraction of total active neurons detected in each brain area. (E) Fraction of total spikes participating in single-cell bursts in each brain area. (F) Fraction of total cells participating in collective bursts in each brain area. (G) Burst amplitude in each brain area, measured as the increase of spikes (events) per second compared to basal spike activity. For A-G datasets: unpaired t-tests, each single point represents an individual, the central line represents the mean, the darker bar the 95% confidence interval and the lighter bar the standard deviation. (H) Principal component analysis of the neuronal activity in the medulla oblongata (MO). The central line represents the mean and the coloured shadow represents the 95% confidence interval. * p < 0.05, ** p < 0.01. YWHAZ, *ywhaz*$^{-/-}$ larvae; WT, wild-type larvae. n= 10 WT and 9 *ywhaz*$^{-/-}$.

Single-cell activity analysis (Supplementary Figure 6) showed that a lower fraction of total spikes participated in single-cell bursts in the MO of *ywhaz*$^{-/-}$ fish (p = 0.039, Figure 3E). In addition, collective burst analysis (Supplementary Figure 7) determined that a lower fraction of MO neurons participate in collective bursts in *ywhaz*$^{-/-}$ fish (p = 0.016, Figure 3F), and that the

collective burst amplitude in MO and tectum is lower in *ywhaz*$^{-/-}$ fish (p = 0.006 for MO and p = 0.043 for tectum, Figure 3G). Finally, a principal component analysis (PCA) demonstrated that a higher number of components is needed to explain variance in neuronal activity in MO of *ywhaz*$^{-/-}$ fish, pointing to a lower neuronal synchronization in this area in mutants (p = 0.005, Figure 3H and Supplementary Figure 8). We then explored possible alterations in connectivity inside each of the defined areas (Supplementary Figure 9). We found a higher clustering coefficient (p = 0.022, Figure 4A) and a higher global efficiency (p = 0.044, Figure 4B) in cerebellum of *ywhaz*$^{-/-}$ fish. Also, we observed a higher assortativity (p = 0.001, Figure 4C) and a higher Louvain community statistic in MO of *ywhaz*$^{-/-}$fish (p = 0.010, Figure 4D). Finally, analyses of connectivity distribution showed that in the MO of WT fish there is a subpopulation of highly connected neurons (connected with 30-40% of the MO neurons) that is not present in the MO of *ywhaz*$^{-/-}$ fish, but no differences were found in cerebellum (Figure 4E and F).

All together, these results point to a higher clustering and more effective connectivity in the cerebellum of *ywhaz*$^{-/-}$fish, and to the presence of more isolated neuronal communities in the MO of *ywhaz*$^{-/-}$fish, which generates a lower collective burst activity and synchrony in this area. Spontaneous synchronized neuronal communication plays an important role during early development in establishing the mature brain circuitry, not only in humans but also in other vertebrates including zebrafish [25–28]. We hypothesize that the alterations in this spontaneous activity may affect neuronal migration and wiring and have a long-term impact in neurotransmission.

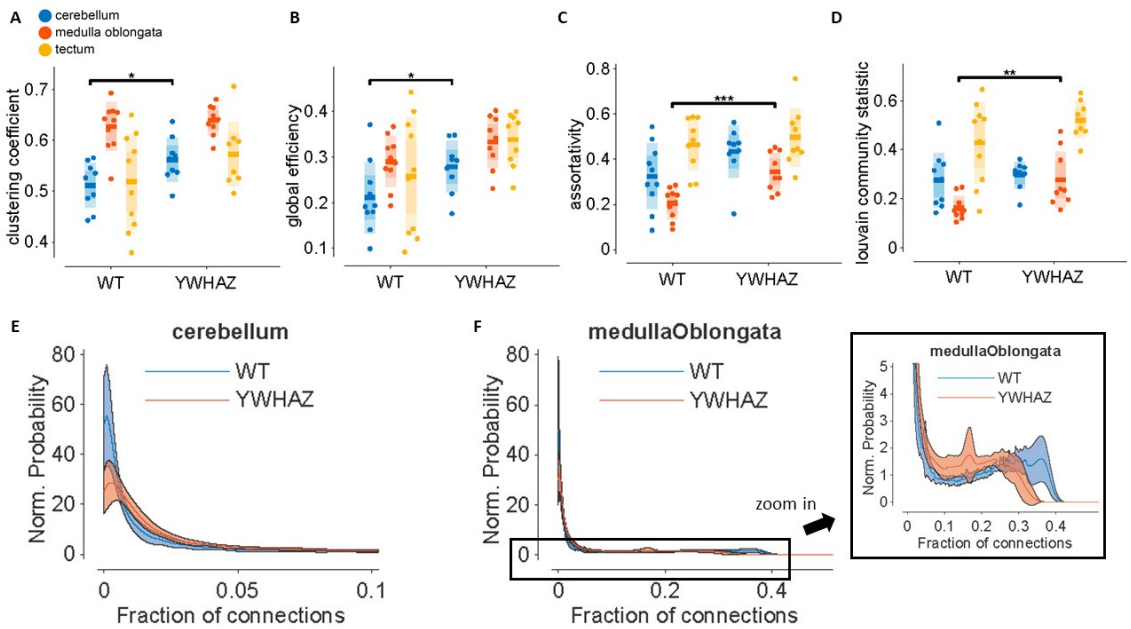

Figure 4. Alterations in neuronal connectivity in zebrafish ywhaz$^{-/-}$ larvae. (A) Normalized clustering coefficient in each brain area. (B) Global efficiency in each brain area. (C) Assortativity in each brain area. (D) Louvain community

statistic in each brain area. For A-D datasets: unpaired t-tests, each single point represents an individual, the central line represents the mean, the darker bar the 95% confidence interval and the lighter bar the standard deviation. (E) No significant differences were found in the connectivity distribution in the cerebellum of WT and *ywhaz*$^{-/-}$ larvae. (F) Connectivity distribution in the medulla oblongata (MO) of WT and *ywhaz*$^{-/-}$ larvae. A subpopulation of highly connected neurons exists in the MO of WT larvae that is absent in *ywhaz*$^{-/-}$ larvae. For E and F: the central line represents the mean and the coloured shadow represents the 95% confidence interval. YWHAZ, *ywhaz*$^{-/-}$ larvae; WT, wild-type larvae. n= 10 WT and 9 *ywhaz*$^{-/-}$. * $p < 0.05$, ** $p < 0.01$, *** $p < 0.001$.

Analysis of monoamines and their metabolites levels

We next investigated whether the observed alterations in neural activity and connectivity caused by a loss of function of *ywhaz* gene during development might affect neurotransmitter signalling in adults. We performed HPLC to measure the basal levels of several neurotransmitters: DOPAC, DA, 5HIAA and 5-HT, in the brain of *ywhaz*$^{-/-}$ and WT adult fish. We found a significant reduction of DA and 5-HT levels in the hindbrain of *ywhaz*$^{-/-}$ ($p = 0.0063$ and $p = 0.0026$ respectively, Figure 5A). No further alterations were found in other areas of the brain (Supplementary Figure 10A-C) nor in the breakdown of 5-HT to 5-hydroxyindoleacetic acid (5HIAA), or dopamine to homovanillic acid (HVA) and dihydroxyphenolacetic acid (DOPAC) (Supplementary Figure 10D-E).

Effects of loss of *ywhaz* function on gene expression

The reduced levels of DA and 5-HT in mutants suggests that *ywhaz* may influence the synthesis of these neurotransmitters. Tyrosine hydroxylase (TH) and Tryptophan hydroxylase (TPH), rate-limiting enzymes in the biosynthesis of DA, are known to be regulated by 14-3-3 proteins [29]. We therefore first measured the expression of genes coding for the DA and 5-HT synthesis enzymes TH and TPH in adult fish. There was an increase in *tryptophan hydroxylase 2* (*tph2*) and tyrosyne hydroxylase 1 (*th1*) expression in *ywhaz*$^{-/-}$ compared to WT, although differences in *th1* did not overcome multiple test corrections. *tph1a*, *tph1b* and *th2* showed all a low expression in both genotypes (Figure 5A). We further examined the transcription of genes coding for proteins involved in the dopaminergic neurotransmitter pathway: the *dopamine transporter solute carrier family 6 member 3* (*slc6a3*), *dopamine receptor 1* (*drd1*), *dopamine receptor 2a* (*drd2a*), *dopamine receptor 2b* (*drd2b*) and *dopamine receptor 4* (*drd4*). The expression of the two isoforms *drd2a and drd2b* was significantly increased in *ywhaz*$^{-/-}$ compared to WT (Figure 5A).

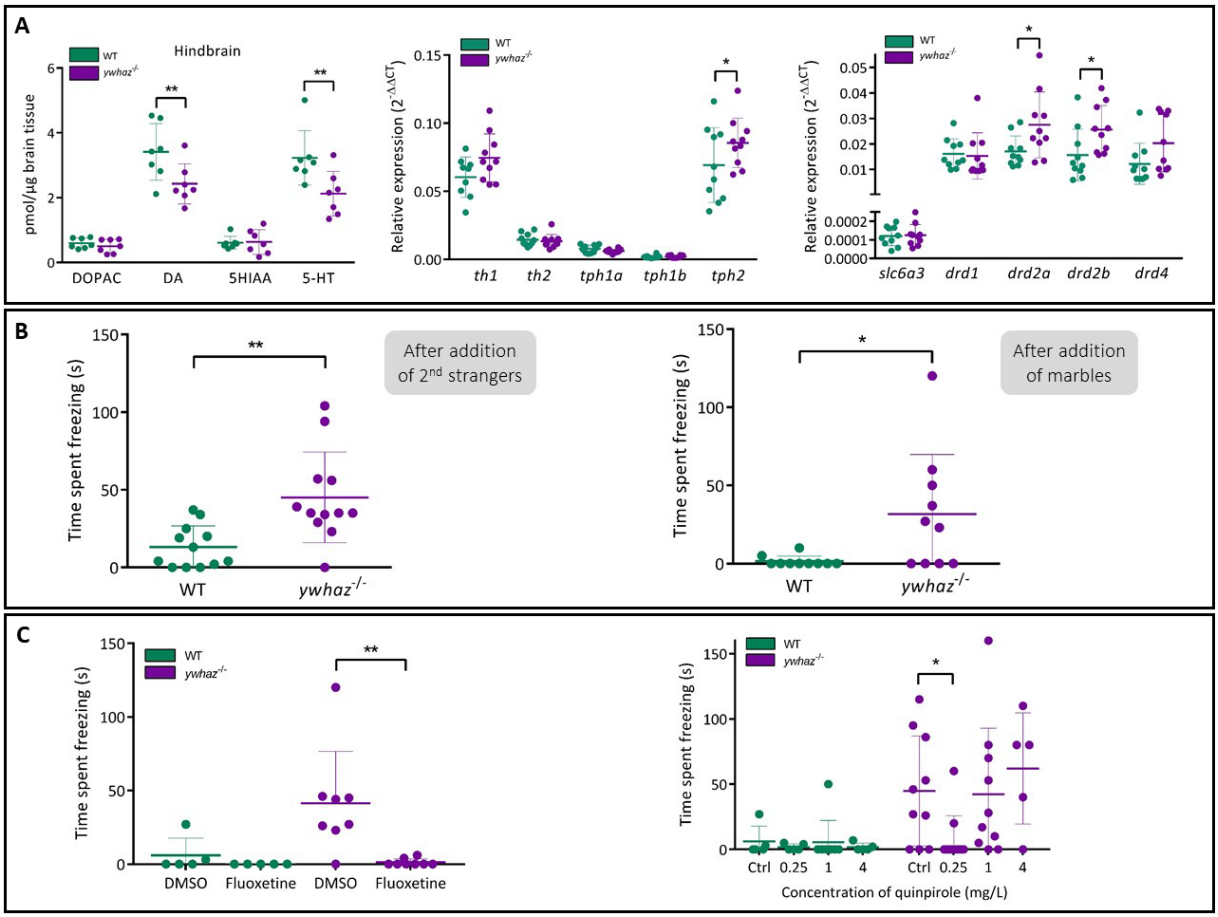

Figure 5. Alterations in the monoamine neurotransmission in the hindbrain of adult KO. (A) On the left, high precision liquid chromatography in the hindbrain of WT and *ywhaz*$^{-/-}$ adult zebrafish. DA and 5-HT levels are decreased in the hindbrain of *ywhaz*$^{-/-}$ compared to WT. DA, dopamine; DOPAC, 3,4-dihydroxyphenylacetic acid; 5-HIAA, 5-hydroxyindoleacetic acid; 5-HT, 5-hydroxytryptamine. n = 7 WT, n = 7 ywhaz$^{-/-}$. In the middle, relative expression profile of *tyrosine hydroxylase 1* (*th1*), *tyrosine hydroxylase 2* (*th2*), *tryptophan hydroxylase 1a* (*tph1a*), *tryptophan hydroxylase 1b* (*tph1b*) and *tryptophan hydroxylase* 2 (*tph2*), normalised to the reference gene ribosomal protein L13 (*rpl13*). *ywhaz*$^{-/-}$ fish have an increased level of *tph2* expression. n = 10 WT, n = 10 *ywhaz*$^{-/-}$. On the right, relative expression profile *of solute carrier family 6 (neurotransmitter transporter), member 3* (*slc6a3*), *dopamine receptor 1* (*drd1*), *dopamine receptor 2a* (*drd2a*), *dopamine receptor 2b* (*drd2b*) and *dopamine receptor 4* (*drd4*), normalised to the reference gene *elongation factor 1a* (*elf1a*). *ywhaz*$^{-/-}$ have an increased level of *drd2a* and *drd2b* expression. n = 10 WT, n = 10 *ywhaz*$^{-/-}$. Multiple t-tests with Holm-Sidak correction for multiple comparisons. (B) Time spent freezing during the first two minutes after the addition of the second group of strangers or marbles in the behavioural setup during the second step of the visually mediated social preference test. Strangers: Unpaired t-test with Welch's correction; n = 12. Marbles: Mann-Whitney U test; n = 10. (C) Treatment with 5 mg/L fluoxetine and 0.25 mg/L quinpirole rescues the freezing phenotype in *ywhaz*$^{-/-}$. On the left, time spent freezing after the addition of the second group of unfamiliar fish in WT or *ywhaz*$^{-/-}$ fish treated with 5 mg/L fluoxetine or DMSO. Multiple t-tests with Holm-Sidak correction for multiple comparisons. n = 5 WT, n = 8 *ywhaz*$^{-/-}$. On the right, time spent freezing after the addition of the second group of unfamiliar fish in WT or *ywhaz*$^{-/-}$ fish treated with different concentrations of quinpirole. Kruskal-Wallis test with Dunn's multiple comparisons. n = 5 WT and n = 10 *ywhaz*$^{-/-}$ for Ctrl, 0.25 mg/L and 1 mg/L; and n = 5 *ywhaz*$^{-/-}$ for 4 mg/L. ** $p < 0.01$, * $p < 0.05$. Mean ± standard deviation.

Pharmacological reversion of *ywhaz*$^{-/-}$ altered behavioural phenotype

A battery of behavioural tests was performed in adult WT and *ywhaz*$^{-/-}$ mutants to characterize possible alterations in behaviour due to *ywhaz* deficiency (Supplementary Figure 11). We only found differences between genotypes in the visually-mediated social preference (VMSP) test, used to assess social behaviour. During the social preference step, both genotypes spent most of the time swimming close to the first group of strangers ($p < 0.0001$ for both WT and *ywhaz*$^{-/-}$; Supplementary Figure 11D). However, during the preference for social novelty step, WT switched preference to the second group of unfamiliar fish ($p = 0.0475$, Supplementary Figure 11D) whereas *ywhaz*$^{-/-}$ fish did not show preference between the two groups of strangers ($p = 0.98$, Supplementary Figure 11D). Instead, we found that immediately after the addition of the second group of unfamiliar fish, *ywhaz*$^{-/-}$ mutants froze significantly more than WT ($p = 0.0035$; Figure 5B). To test whether it was the live stimulus that caused this phenotype, we repeated the test by adding marbles instead of the second group of unfamiliar fish and observed the same freezing behaviour in *ywhaz*$^{-/-}$ mutants ($p = 0.0251$, Figure 5B). Contrary to adults, juvenile ywhaz$^{-/-}$ fish did not show an altered social behaviour: they did not show any increase in freezing behaviour in the VMSP test ($p > 0.99$, Supplementary Figure 12A-C), nor an altered cluster score in the shoaling test for social interaction in a group (Supplementary Figure 12D).

HPLC and qPCR results suggested that alterations to 5-HT and DA signalling may underlie the behavioural phenotype of ywhaz$^{-/-}$. We therefore used fluoxetine, a selective serotonin reuptake inhibitor (SSRI) [30], and quinpirole, a selective D2-like receptor agonist [31] to investigate the connection between 5-HT, DA, and the behavioural phenotype observed in *ywhaz*$^{-/-}$ in the VMSP test. Treatment with 5 mg/L fluoxetine and treatment with 0.25 mg/L quinpirole significantly decreased the time *ywhaz*$^{-/-}$ spent freezing after the addition of the second group of unfamiliar fish ($p = 0.006$ and $p= 0.0468$, respectively, Figure 5C) without affecting WT behaviour. However, a higher concentration of quinpirole, 1 or 4 mg/L, did not reverse the freezing behaviour ($p > 0.99$ for both concentrations, Figure 5C).

Several behavioural tests were repeated in a second group of adult fish and an increased freezing behaviour was observed in ywhaz$^{-/-}$ fish in all the tests performed (Supplementary Figure 13). Additionally, a third batch of behavioural tests was performed in a different setup, but strong differences in the WT behaviour of this batch, probably due to environmental effects, prevent us from comparing the results obtained in this batch with the previous batches (Supplementary Figure 14).

DISCUSSION

Functional and genetic studies had previously suggested a role of *YWHAZ* gene in neurodevelopmental disorders such as ASD or schizophrenia [2, 5, 6, 32]. In this study, we have used zebrafish to investigate *ywhaz* function in neural development and adult behaviour. We found that *ywhaz* deficiency resulted in an altered hindbrain connectivity during larval stages and a neurotransmitter imbalance during adulthood leading to alterations in behaviour.

We observed a pan-neuronal expression of *ywhaz* in larval stages, which suggests that *ywhaz* may be involved in a wide range of functions during zebrafish neurodevelopment. Indeed, the important function of *Ywhaz* in neurogenesis and neuronal differentiation was previously demonstrated in mice KO models [1–5], and disrupted neurogenesis is a known risk factor for neurodevelopmental disorders [33]. Although expressed pan-neuronally, *ywhaz* presents a stronger expression in larvae cerebellum, a brain region whose dysfunction has been related to neurodevelopmental disorders [34, 35]. Interestingly, a decreased *YWHAZ* expression was reported in the cerebellum of ASD patients [6]. In adults, *ywhaz* is specifically expressed in Purkinje cells (PC) in the cerebellum. Post-mortem studies have shown a reduction in PC density in the brain of autistic patients, and *Tsc1* mutant mice with a decrease in PC functioning show autistic-like behaviours [36, 37]. *ywhaz* is therefore expressed in brain regions that play a crucial role in neurodevelopment and whose dysfunction is related to neurodevelopmental disorders.

Early spontaneous synchronized burst activity is essential for the correct assembly of neural circuits during development [25, 38]. Indeed, neuronal activity controls apoptosis and future connectivity in the developing cortex of mice [39], and a recent article reviewed the relevance of spontaneous activity in the larval zebrafish optic tectum and its implication in the response to sensory information [26]. In addition, magnetic resonance studies have described an altered functional connectivity in patients diagnosed with ASD or schizophrenia [40–44]. Here, *ywhaz*$^{-/-}$ larvae present a decreased burst activity and synchronization in the hindbrain, the region where *ywhaz* showed a higher expression in WT animals. We then identified decreased levels of DA and 5-HT in the hindbrain of *ywhaz*$^{-/-}$ adults, suggesting long-term alterations in brain function. These findings suggest that *ywhaz* is involved in establishing brain connectivity during development and that this impaired connectivity may contribute to the subsequent neurotransmitter alterations found in adults.

Among all 14-3-3 isoforms, *YWHAZ* plays the most important role in DA synthesis [45]. Indeed, *YWHAZ* is known to regulate the function of TH and TPH, rate-limiting enzymes in the biosynthesis of DA [29]. In a previous work, we demonstrated that a disrupting mutation in

YWHAZ produced the loss of affinity of the protein for TH [6]. Therefore, *ywhaz* deficiency may contribute to a decrease in TH activity and a subsequent reduction in DA levels. These results are in line with the alterations in DA system previously reported in patients with neurodevelopmental disorders such as ASD, ADHD or schizophrenia [46–48]. The increased *drd2a* and *drd2b* levels we reported in *ywhaz* mutants may be due to compensatory mechanisms to overcome DA depletion. Interestingly, schizophrenia patients have a higher density of DRD2 receptors and all antipsychotic drugs used today are DRD2 antagonists [49, 50]. In addition, upregulation of *tph2* may be a mechanism to compensate for the depletion of 5-HT we found in the hindbrain of *ywhaz*$^{-/-}$ adults. In line with these results, altered levels of 5-HT have been reported in ASD and schizophrenia patients [51, 52].

Finally, treatment with fluoxetine, a serotonin reuptake inhibitor, and quinpirole, a selective DRD2-like receptor agonist, were able to rescue the abnormal neophobic freezing behaviour observed in *ywhaz* mutants. Similarly, in a previous study, behavioural alterations were rescued in *Ywhaz*$^{-/-}$ mice using the antipsychotic drug clozapine, an antagonist of DA and 5-HT receptors used as a medication for schizophrenia [53]. 5-HT and DA are involved in sensory processing and social cognition [54, 55], and DA plays an important role in social reward [56]. Given 5-HT and DA function in behaviour, we hypothesize that 5-HT and DA alterations in mutant fish are responsible for the exaggerated response to novel stimuli present in *ywhaz*$^{-/-}$ adults.

Several strengths and limitations of this study should be discussed. First, whole-brain imaging experiments were performed in 6 dpf larvae whereas neurotransmitter levels and behaviour were investigated in adult fish, due to the impossibility of performing all these experiments at the same age. Even though this constitutes a limitation, it brings useful complementary information to analyse the effect of *ywhaz* deficiency at different levels and ages. In addition, our whole-brain imaging setup did not permit us to analyse neuronal activity in ventral brain regions. Therefore, it would be interesting to perform similar imaging recordings in an adapted setup that allows to scan deep brain areas and to analyse brain activity in response to stimuli. Finally, the differences observed in the behavioural phenotype between batches of experiments may be due to environmental differences (between setups) and to (epi)genetic changes between fish generations. Indeed, a previous study reported differences between *Ywhaz*$^{-/-}$ mice with a different genetic background [2], and it is well described that environment plays an important role in the onset or phenotypical expression of psychiatric and neurodevelopmental disorders.

In conclusion, our findings highlight the important role of *YWHAZ* in neurodevelopment and shed light on the neurobiological mechanisms underlying its contribution to

neurodevelopmental disorders. Pharmacological recovery of altered behaviour of *ywhaz*$^{-/-}$ fish provide some clues for the use of specific treatments to revert the associated symptomatology to neuropsychiatric disorders, such as ASD or schizophrenia.

REFERENCES

1. Cornell B, Toyo-oka K. 14-3-3 proteins in brain development: Neurogenesis, neuronal migration and neuromorphogenesis. Front Mol Neurosci. 2017;10:318.
2. Xu X, Jaehne EJ, Greenberg Z, McCarthy P, Saleh E, Parish CL, et al. 14-3-3ζ deficient mice in the BALB/c background display behavioural and anatomical defects associated with neurodevelopmental disorders. Sci Rep. 2015;5:12434.
3. Toyo-Oka K, Wachi T, Hunt RF, Baraban SC, Taya S, Ramshaw H, et al. 14-3-3E and Z Regulate Neurogenesis and Differentiation of Neuronal Progenitor Cells in the Developing Brain. J Neurosci. 2014;34:12168–12181.
4. Jaehne EJ, Ramshaw H, Xu X, Saleh E, Clark SR, Schubert KO, et al. In-vivo administration of clozapine affects behaviour but does not reverse dendritic spine deficits in the 14-3-3ζ KO mouse model of schizophrenia-like disorders. Pharmacol Biochem Behav. 2015;138:1–8.
5. Cheah PS, Ramshaw HS, Thomas PQ, Toyo-Oka K, Xu X, Martin S, et al. Neurodevelopmental and neuropsychiatric behaviour defects arise from 14-3-3ζ deficiency. Mol Psychiatry. 2012;17:451–466.
6. Torrico B, Antón-Galindo E, Fernàndez-Castillo N, Rojo-Francàs E, Ghorbani S, Pineda-Cirera L, et al. Involvement of the 14-3-3 Gene Family in Autism Spectrum Disorder and Schizophrenia: Genetics, Transcriptomics and Functional Analyses. J Clin Med. 2020;9:1851.
7. Jia Y, Yu X, Zhang B, Yuan Y, Xu Q, Shen Y, et al. An association study between polymorphisms in three genes of 14-3-3 (tyrosine 3-monooxygenase/tryptophan 5-monooxygenase activation protein) family and paranoid schizophrenia in northern Chinese population. Eur Psychiatry. 2004;19:377–379.
8. Middleton FA, Peng L, Lewis DA, Levitt P, Mirnics K. Altered expression of 14-3-3 in the prefrontal cortex of subjects with schizophrenia. Neuropsychopharmacology. 2005;30:974–983.
9. English JA, Pennington K, Dunn MJ, Cotter DR. The neuroproteomics of schizophrenia. Biol Psychiatry. 2011;69:163–172.
10. Pagan C, Delorme R, Callebert J, Goubran-Botros H, Amsellem F, Drouot X, et al. The serotonin-N-acetylserotonin-melatonin pathway as a biomarker for autism spectrum disorders. Transl Psychiatry. 2014;4:e479.
11. Pagan C, Goubran-Botros H, Delorme R, Benabou M, Lemière N, Murray K, et al. Disruption of melatonin synthesis is associated with impaired 14-3-3 and miR-451 levels in patients with autism spectrum disorders. Sci Rep. 2017;7:2096.
12. Kalueff A V., Stewart AM, Gerlai R. Zebrafish as an emerging model for studying complex brain disorders. Trends Pharmacol Sci. 2014;35:63–75.
13. Norton W. Towards developmental models of psychiatric disorders in zebrafish. Front Neural Circuits. 2013;7:1–12.
14. Ahrens MB, Orger MB, Robson DN, Li JM, Keller PJ. Whole-brain functional imaging at cellular resolution using light-sheet microscopy. Nat Methods. 2013;10:413–420.
15. Vanwalleghem GC, Ahrens MB, Scott EK. Integrative whole-brain neuroscience in larval zebrafish. Curr Opin Neurobiol. 2018;50:136–145.
16. Hwang WY, Fu Y, Reyon D, Maeder ML, Tsai SQ, Sander JD, et al. Efficient genome editing in zebrafish using a CRISPR-Cas system. Nat Biotechnol. 2013;31:227–229.
17. Giovannucci A, Friedrich J, Gunn P, Kalfon J, Brown BL, Koay SA, et al. CaImAn an open source tool for scalable calcium imaging data analysis. Elife. 2019;8:1–45.
18. Pnevmatikakis EA, Soudry D, Gao Y, Machado TA, Merel J, Pfau D, et al. Simultaneous Denoising, Deconvolution, and Demixing of Calcium Imaging Data. Neuron. 2016;89:285.
19. Young AMJ. Increased extracellular dopamine in nucleus accumbens in response to unconditioned and

conditioned aversive stimuli: Studies using 1 min microdialysis in rats. J Neurosci Methods. 2004;138:57–63.

20. Ahn AH, Dziennis S, Hawkes R, Herrup K. The cloning of zebrin II reveals its identity with aldolase C. Development. 1994;120:2081–2090.

21. McFarland KA, Topczewska JM, Weidinger G, Dorsky RI, Appel B. Hh and Wnt signaling regulate formation of olig2+ neurons in the zebrafish cerebellum. Dev Biol. 2008;318:162–171.

22. Hibi M, Shimizu T. Development of the cerebellum and cerebellar neural circuits. Dev Neurobiol. 2012;72:282–301.

23. Biechl D, Dorigo A, Köster RW, Grothe B, Wullimann MF. Eppur Si muove: Evidence for an external granular layer and possibly transit amplification in the teleostean cerebellum. Front Neuroanat. 2016;10.

24. Karousis ED, Nasif S, Mühlemann O. Nonsense-mediated mRNA decay: novel mechanistic insights and biological impact. Wiley Interdiscip Rev RNA. 2016;7:661–682.

25. Molnár Z, Luhmann HJ, Kanold PO. Transient cortical circuits match spontaneous and sensory-driven activity during development. Science (80-). 2020;370.

26. Marachlian E, Avitan L, Goodhill GJ, Sumbre G. Principles of functional circuit connectivity: Insights from spontaneous activity in the zebrafish optic tectum. Front Neural Circuits. 2018;12:1–8.

27. Avitan L, Pujic Z, Mölter J, Van De Poll M, Sun B, Teng H, et al. Spontaneous Activity in the Zebrafish Tectum Reorganizes over Development and Is Influenced by Visual Experience. Curr Biol. 2017;27:2407-2419.e4.

28. Momose-Sato Y, Sato K. Development of spontaneous activity in the avian hindbrain. Front Neural Circuits. 2016;10:1–8.

29. Aitken A. 14-3-3 proteins: A historic overview. Semin Cancer Biol. 2006;16:162–172.

30. Vaswani M, Linda FK, Ramesh S. Role of selective serotonin reuptake inhibitors in psychiatric disorders: A comprehensive review. Prog Neuro-Psychopharmacology Biol Psychiatry. 2003;27:85–102.

31. Millan MJ, Maiofiss L, Cussac D, Audinot V, Boutin JA, Newman-Tancredi A. Differential actions of antiparkinson agents at multiple classes of monoaminergic receptor. I. A multivariate analysis of the binding profiles of 14 drugs at 21 native and cloned human receptor subtypes. J Pharmacol Exp Ther. 2002;303:791–804.

32. Toma C, Torrico B, Hervás A, Valdés-Mas R, Tristán-Noguero A, Padillo V, et al. Exome sequencing in multiplex autism families suggests a major role for heterozygous truncating mutations. Mol Psychiatry. 2014;19:784–790.

33. Packer A. Neocortical neurogenesis and the etiology of autism spectrum disorder. Neurosci Biobehav Rev. 2016;64:185–195.

34. Stoodley CJ. The Cerebellum and Neurodevelopmental Disorders. Cerebellum. 2016;15:34–37.

35. van der Heijden ME, Gill JS, Sillitoe R V. Abnormal Cerebellar Development in Autism Spectrum Disorders. Dev Neurosci. 2021:1–10.

36. Tsai PT, Hull C, Chu Y, Greene-Colozzi E, Sadowski AR, Leech JM, et al. Autistic-like behaviour and cerebellar dysfunction in Purkinje cell Tsc1 mutant mice. Nature. 2012;488:647–651.

37. Skefos J, Cummings C, Enzer K, Holiday J, Weed K, Levy E, et al. Regional Alterations in Purkinje Cell Density in Patients with Autism. PLoS One. 2014;9:e81255.

38. Kirkby LA, Sack GS, Firl A, Feller MB. A role for correlated spontaneous activity in the assembly of neural circuits. Neuron. 2013;80:1129–1144.

39. Blanquie O, Yang JW, Kilb W, Sharopov S, Sinning A, Luhmann HJ. Electrical activity controls area-specific expression of neuronal apoptosis in the mouse developing cerebral cortex. Elife. 2017;6:1–21.

40. O'Reilly C, Lewis JD, Elsabbagh M. Is functional brain connectivity atypical in autism? A systematic review of EEG and MEG studies. PLoS One. 2017;12:1–28.

41. Rane P, Cochran D, Hodge SM, Haselgrove C, Kennedy DN, Frazier JA. Connectivity in Autism: A Review of MRI Connectivity Studies. Harv Rev Psychiatry. 2015;23:223–244.

42. Li X, Zhang K, He X, Zhou J, Jin C. Structural , Functional , and Molecular Imaging of Autism Spectrum Disorder. Neurosci Bull. 2021. 2021. https://doi.org/10.1007/s12264-021-00673-0.

43. Sheffield JM, Barch DM. Cognition and resting-state functional connectivity in schizophrenia. Neurosci Biobehav Rev. 2016;61:108–120.

44. Van Den Heuvel MP, Fornito A. Brain networks in schizophrenia. Neuropsychol Rev. 2014;24:32–48.

45. Wang J, Lou H, Pedersen CJ, Smith AD, Perez RG. 14-3-3ζ contributes to tyrosine hydroxylase activity in MN9D cells: Localization of dopamine regulatory proteins to mitochondria. J Biol Chem. 2009;284:14011–14019.

46. Kesby JP, Eyles DW, McGrath JJ, Scott JG. Dopamine, psychosis and schizophrenia: The widening gap between basic and clinical neuroscience. Transl Psychiatry. 2018;8:30.

47. Pavăl D. A Dopamine Hypothesis of Autism Spectrum Disorder. Dev Neurosci. 2017;39:355–360.

48. Tripp G, Wickens JR. Neurobiology of ADHD. Neuropharmacology. 2009;57:579–589.

49. Zakzanis KK, Hansen KT. Dopamine D2 densities and the schizophrenic brain. Schizophr Res. 1998;32:201–206.

50. Kestler LP, Walker E, Vega EM. Dopamine receptors in the brains of schizophrenia patients: A meta-analysis of the findings. Behav Pharmacol. 2001;12:355–371.

51. Gabriele S, Sacco R, Persico AM. Blood serotonin levels in autism spectrum disorder: A systematic review and meta-analysis. Eur Neuropsychopharmacol. 2014;24:919–929.

52. Muck-Seler D, Pivac N, Mustapic M, Crncevic Z, Jakovljevic M, Sagud M. Platelet serotonin and plasma prolactin and cortisol in healthy, depressed and schizophrenic women. Psychiatry Res. 2004;127:217–226.

53. Ramshaw H, Xu X, Jaehne EJ, McCarthy P, Greenberg Z, Saleh E, et al. Locomotor hyperactivity in 14-3-3ζ KO mice is associated with dopamine transporter dysfunction. Transl Psychiatry. 2013;3:e327.

54. Jacob SN, Nienborg H. Monoaminergic Neuromodulation of Sensory Processing. Front Neural Circuits. 2018;12:1–17.

55. Fernández M, Mollinedo-Gajate I, Peñagarikano O. Neural Circuits for Social Cognition: Implications for Autism. Neuroscience. 2018;370:148–162.

56. Rademacher L, Schulte-Rüther M, Hanewald B, Lammertz S. Reward: From basic reinforcers to anticipation of social cues. Curr. Top. Behav. Neurosci., vol. 30, Springer Verlag; 2016. p. 207–221.